Available online at www.sciencedirect.com
ScienceDirect
Journal of Power Sources 168 (2007) 111–118
JOURNAL OF POWER SOURCES
www.elsevier.com/locate/jpowsour

Evaluation of carbon materials for use in a direct carbon fuel cell

Gregory A. Hackett [a,*], John W. Zondlo [a], Robert Svensson [b]

[a] *Department of Chemical Engineering, West Virginia University, Engineering Sciences Building, Room 403, Morgantown, WV, United States*
[b] *Department of Biomedical Engineering, Chalmers University of Technology, Göteborg, Sweden*

Received 21 December 2006; received in revised form 2 February 2007; accepted 5 February 2007
Available online 21 February 2007

Abstract

The direct carbon fuel cell (DCFC) employs a process by which carbon is converted to electricity, without the need for combustion or gasification. The operation of the DCFC is investigated with a variety of solid carbons from several sources including some derived from coal. The highly organized carbon form, graphite, is used as the benchmark because of its availability and stability. Another carbon form, which is produced at West Virginia University (WVU), uses different mixtures of solvent extracted carbon ore (SECO) and petroleum coke. The SECO is derived from coal and both this and the petroleum coke are low in ash, sulfur, and volatiles. Compared to graphite, the SECO is a less-ordered form of carbon. In addition, GrafTech, Inc. (Cleveland, OH) supplied a well-fabricated baked carbon rod derived from petroleum coke and conventional coal–tar binder. The open-circuit voltage of the SECO rod reaches a maximum of 1.044 V while the baked and graphite rods only reach 0.972 V and 0.788 V, respectively. With this particular cell design, typical power densities were in the range of 0.02–0.08 W cm^{-2}, while current densities were between 30 and 230 mA cm^{-2}. It was found that the graphite rod provided stable operation and remained intact during multi-hour test runs. However, the baked (i.e., non-graphitized) rods failed after a few hours due to selective attack and reaction of the binder component.

Keywords: Direct carbon fuel cell; DCFC; Carbon; Graphite; Coal; Coal rods

1. Introduction

Coal is the most abundant fossil fuel in the United States. The dependence upon coal as a fuel source continues to be widespread, as other natural resources remain in short supply. In 2004, West Virginia mines produced over 153 million tonnes of coal [1]. Therefore, it is logical to investigate a new process in which coal is used as a carbon source for direct conversion to electricity.

The direct carbon fuel cell (DCFC) has the potential to convert the chemical energy of carbon directly into electricity without the need for gasification or the moving machinery associated with conventional electric generators. Moreover, these fuel cells could be twice as fuel-efficient as coal-fired power plants, resulting in reduced carbon dioxide emissions per unit of generated electricity. These advantages, and the favorable thermodynamics of direct oxidation, result in thermodynamic efficiencies up to 80% [2]. The process produces a concentrated carbon dioxide stream, which can be easily collected for downstream disposal using methods such as carbon sequestration. Carbon is not reacted at high temperatures, therefore, the exhaust is free of thermal nitrogen oxides (NO_x), eliminating many pollution issues caused by conventional coal combustion.

Because of the absence of a need for smoke stacks, direct carbon fuel cells can easily be located in urban areas. Thus, DCFCs are more environmentally friendly than coal-fired power plants.

2. Background

Sir William Grove first discovered the direct carbon fuel cell in 1839. Since then, researchers have attempted to perfect the invention. The first direct carbon fuel cell, as shown in Fig. 1, was built in 1896 by American Engineer Dr. William W. Jacques, and was very simple and inexpensive. The cell used a steel pot filled with molten sodium hydroxide, through which air was bubbled. A carbon rod was placed into the molten sodium hydroxide electrolyte. The steel pot acted as the air cathode and the carbon rod acted as both the fuel and the anode.

* Corresponding author. Tel.: +1 412 613 2294; fax: +1 304 293 4139.
E-mail address: ghackett@mix.wvu.edu (G.A. Hackett).

0378-7753/$ – see front matter © 2007 Published by Elsevier B.V.
doi:10.1016/j.jpowsour.2007.02.021

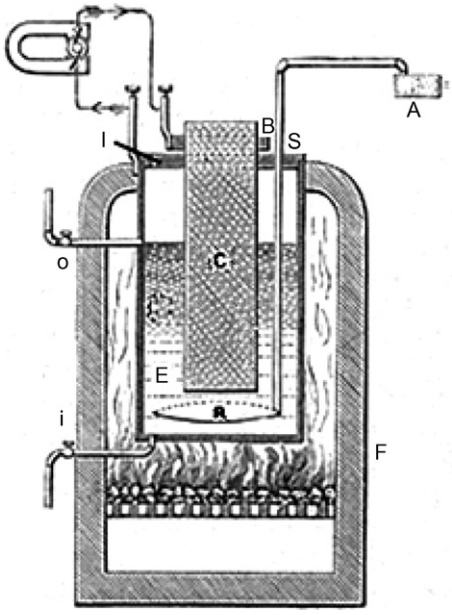

Fig. 1. Line art depicting Dr. Jacques' direct carbon fuel cell [3].

Experiments conducted by Jacques included several different cells, electrolytes, and cathode materials. He then placed his most successful trials in a series of about 100 cells and generated over 1 kW of electricity. The series produced a current density of 100 mA cm^{-2} at 1 VDC. It was also the first DCFC to be operated long term [4]. In his patent [3], Jacques claimed an efficiency of 82%; however, reviewers concluded that he had neglected thermal energy requirements for heating the electrolyte and the power needed to run his air pump. Their much-debated conclusion showed an overall efficiency of only 8%. Even so, the cell stack did indeed produce over a kilowatt of electricity.

In the early 1970s during the oil crisis, the Stanford Research Institute (SRI, Menlo Park, CA) was funded to complete a carbon fuel cell. The research leader, Dr. Robert Weaver, was successful in proving that the electrochemical oxidation of carbon is feasible. The research group later tested several different types of carbons [5]. As shown in Fig. 2, the group was able to demonstrate that a coal-derived anode was much more electrochemically active (i.e., gave a larger potential, as shown as a more negative voltage in Fig. 2) than a graphite anode.

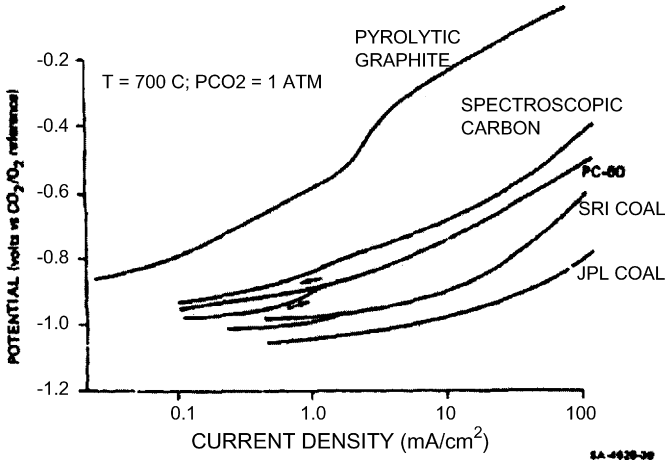

Fig. 2. Performance of various carbons in a direct carbon fuel cell [6].

The element carbon has an affinity for combining electrically with a large number of other chemical elements under a variety of conditions. In the DCFC, the exothermic reaction of carbon and oxygen is used to provide the necessary electrons from the system. Using a hydroxide electrolyte, the chemical reactions that occur with a carbon-based fuel in the DCFC are as follows:

$$C + O_2 \rightarrow CO_2 \quad (1)$$

$$C + 4OH^- \rightarrow CO_2 + 2H_2O + 4e^- \quad (2)$$

$$4e^- + O_2 + 2H_2O \rightarrow 4OH^- \quad (3)$$

$$CO_2 + 2OH^- \rightarrow CO_3^{2-} + H_2O \quad (4)$$

Eq. (1) is the overall reaction, and is the direct oxidation of carbon. Eq. (2) is the reaction between the carbon fuel and the molten hydroxide electrolyte that occurs at the anode, showing that four electrons are produced per atom of carbon. Eq. (3) represents the cathode reaction between the oxygen, water, and electrons that replenishes the hydroxide electrolyte. Moreover, the addition of water vapor increases the ionic conductivity in the electrolyte by adding polar molecules. Eq. (4) is an undesired side reaction that consumes the electrolyte producing the carbonate ion. The occurrence of this reaction is minimized by the addition of excess water vapor, which will hydrolyze the carbonate anion, reforming the previously consumed hydroxide.

3. Experimental

3.1. Direct carbon fuel cell design

A detailed schematic diagram of the designed fuel cell is shown in Fig. 3 with an actual photograph of the fuel cell test stand shown in Fig. 4.

As previously mentioned, the DCFC design, in the most basic sense, consists of a metal cathode and a carbon anode. More specifically, carbon rods are used as the anode while an iron–titanium alloy (98–2%) is used as the cathode. In this case, a molten electrolyte of sodium hydroxide (NaOH) supplies the hydroxide ions necessary for the anode half-reaction (Eq. (2)). The electrolyte is contained by the cathode, which is shaped into a can.

The oxygen supply, air, humidified at 70 °C, is pre-heated to the fuel cell operating temperature (600–700 °C), and then is distributed to the cathode by means of a "spider-type" sparger. The spider takes the air inlet and directs it toward the inner surface area of the can, supplying small bubbles of needed oxygen and water to the cathode half-reaction (Eq. (3)). An inconel wire (0.041 in. OD) is used as a reference electrode for separate anode and cathode voltage measurements. A type-K thermocouple is placed in a ceramic thermal well to measure directly the electrolyte temperature for control purposes.

The fuel cell is heated electrically to the desired operating temperature by means of two 1.25 kW ceramic fiber heaters. The fuel cell and the pre-heated air tubing are well-insulated to help prevent thermal losses.

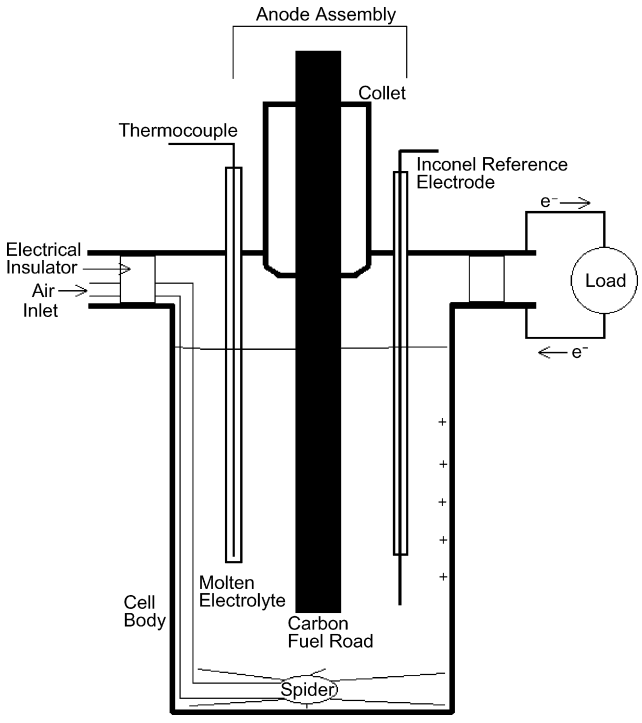

Fig. 3. Schematic diagram of direct carbon fuel cell.

The electrochemical load characteristics of the operating cell were determined by means of an electronic load (TDI, Hackettstown, NJ, model SDL 1103). Both the cell and pre-heater temperatures are controlled by PID controllers (RKC Instruments, South Bend, IN, model REX-P9) and the air flow is set with an electronic mass flow controller (Alicat Scientific, Tucson, AZ, model MC-02SLPM-D).

3.2. Carbon materials discussion and analysis

3.2.1. Graphite fuel rods

The graphite rods were tested in the DCFC to provide a reliable baseline for carbon anode testing. The rods were very well made through an extrusion process at NAC Carbon Products, Inc. (NAC, Punxsutawney, PA, part NAC-500). There were no visible cracks or other defects on these rods. The outer diameter of the graphite rods was 0.5 in.

An elemental analysis of these rods showed that the composition was well over 99% carbon with no detectable hydrogen or sulfur. The resistivity of these rods was also measured and the average was found to be 6.20 μΩ m. This is lower than the coal-derived rods that will be discussed in the following section.

Additional graphitized rods were supplied by GrafTech, Inc. (Cleveland, OH), which specializes in the production of synthetic graphite. The rods produced by GrafTech did not have any visible cracks and had an outer diameter of 0.75 in. The resistivity of these rods was measured and found to be 8.67 μΩ m. The average literature value for graphite is 7.837 μΩ m [7].

3.2.2. Coal-derived fuel rods

The coal-derived rods were made at West Virginia University (WVU) using a combination of solvent extracted carbon ore (SECO), petroleum coke (PetCoke), and a standard coal tar binder pitch which binds the SECO and PetCoke together. The binder pitch was supplied by Koppers, Inc. and had a softening point of approximately 110 °C. SECO is a low-ash extract material that is produced from bituminous coal at WVU by solvent extraction using *N*-methylpyrrolidone as the solvent [8]. Petroleum coke is an anisotropic carbon produced in a delayed coker at the refinery. It has a low electrical resistivity, making it ideal for use as an anode material. Both the PetCoke and the SECO were ground to −120 mesh prior to mixing with the binder pitch. Some of the rods were created as pure PetCoke (no SECO in mixture) at a composition of (80% PetCoke:20% binder pitch). The amount of binder pitch was determined experimentally. These rods were pressed in a heated mold at 200 °C and then calcined to 1000 °C. They were used in Runs #11 and #12, as described in the following section. Other rods were made by the same procedure and included different compositions of SECO and PetCoke, using 15% coal tar binder pitch to hold the mixture together. Analysis of the finished SECO/PetCoke calcined rods is given in Table 1. Details of the production of these rods can be found elsewhere [9].

The WVU baked rods had a higher resistivity than the graphite rods. The resistivities ranged from 53 to 140 μΩ m, which is an order of magnitude larger than the graphite rods. This was a result of both the manufacturing procedure as well as the coke properties. It should be noted that these rods had visible cracks in the surface and had some variation in their quality.

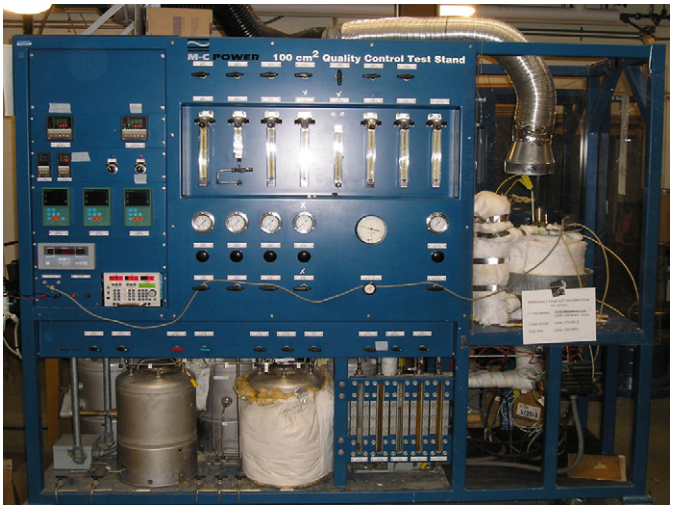

Fig. 4. Photograph of fuel cell test stand.

Table 1
Elemental analysis and ash content for seco/petcoke rods

Coke blend	Nitrogen (%)	Carbon (%)	Hydrogen (%)	Sulfur (%)	Ash (%)
0% SECO, 100% PetCoke	1.22	97.53	0.01	2.01	0.67
25% SECO, 75% PetCoke	1.10	83.70	0.00	0.77	0.62
50% SECO, 50% PetCoke	1.26	87.60	0.00	0.45	0.54
75% SECO, 25% PetCoke	1.22	88.30	0.00	0.24	0.62
100% SECO, 0% PetCoke	1.46	90.80	0.01	0.23	0.54

In order to elucidate the possible connection between the method of manufacture and the rod resistivity, GrafTech, Inc. supplied well-fabricated baked rods for testing. GrafTech used an extrusion-type process to produce these rods. They were made from premium petroleum coke and binder pitch. They were baked at 1000 °C but not graphitized. These rods did not have any visible flaws on the surface. The resistivity of these rods was measured to be 60 μΩ m, similar to the WVU baked rods.

3.3. Experimental design

The main objective of this research was to investigate the effects of different types of carbon-based fuel rods on fuel cell performance [10]. In addition, in some cases, the operating conditions were changed while using the same type of carbon rod. This allowed an assessment of both the effect of the rod type as well as the operating conditions. Most of the experiments were conducted with graphite rods. These rods were tested multiple times to investigate process variables such as air flow rate and fuel cell temperature. The graphite rods were used more extensively than the others because they were commercially available in large quantity.

The experimental design is summarized below:

1. Graphite rod, $T = 600$ °C, air flow = 0.25 SLPM, NaOH electrolyte
2. Graphite rod, $T = 600$ °C, air flow = 0.50 SLPM, NaOH electrolyte
3. Graphite rod, $T = 600$ °C, air flow = 0.75 SLPM, NaOH electrolyte
4. Graphite rod, $T = 600$ °C, air flow = 0.90 SLPM, NaOH electrolyte
5. Graphite rod, $T = 625$ °C, air flow = 0.50 SLPM, NaOH electrolyte
6. Graphite rod, $T = 650$ °C, air flow = 0.50 SLPM, NaOH electrolyte
7. Graphite rod, $T = 675$ °C, air flow = 0.25 SLPM, NaOH electrolyte
8. Graphite rod, $T = 675$ °C, air flow = 0.50 SLPM, NaOH electrolyte
9. Graphite rod, $T = 675$ °C, air flow = 0.75 SLPM, NaOH electrolyte
10. Graphite rod, $T = 700$ °C, air flow = 0.50 SLPM, NaOH electrolyte
11. 100% Petcoke Rod #11, $T = 600$ °C, air flow = 0.50 SLPM, NaOH electrolyte
12. 100% Petcoke Rod #10, $T = 600$ °C, air flow = 0.50 SLPM, NaOH electrolyte
13. 25% SECO, 75% PetCoke rod, $T = 600$ °C, air flow = 0.50 SLPM, NaOH electrolyte
14. 50% SECO, 50% PetCoke rod, $T = 600$ °C, air flow = 0.50 SLPM, NaOH electrolyte
15. 75% SECO, 25% PetCoke rod, $T = 600$ °C, air flow = 0.50 SLPM, NaOH electrolyte
16. 100% SECO, $T = 600$ °C, air flow = 0.50 SLPM, NaOH electrolyte
17. GrafTech graphite rod, $T = 600$ °C, air flow = 0.50 SLPM, NaOH electrolyte
18. GrafTech baked rod, $T = 600$ °C, air flow = 0.50 SLPM, NaOH electrolyte

The carbon rods are different both in their composition and in the way that they were manufactured. The investigation included a good sampling of rods that varied in one or both of these characteristics.

Some of the various experiments were completed during the same experimental run, i.e., the air flow rate and fuel cell temperature were changed during a single experiment. All tests were done with sodium hydroxide electrolyte.

Data were collected after the cell had equilibrated for an hour. Data analysis consisted of plotting the generated cell voltage (V) versus the current density (mA cm^{-2}) that is drawn from the cell using the electronic load, the so-called *i–V* curves. By using the current density, i.e., the current drawn over the surface area of the rod immersed in the electrolyte, the data are normalized for rods of different diameter and surface area. Similarly, the power density is plotted versus the current density to assess the maximum power. Fuel cells are designed to operate at or below the power density maximum. At current densities below the power density maximum, voltage improves but the power density falls. At current densities above the maximum, both voltage and power density fall sharply. The slope of the cell voltage versus the current density in the linear central region of the *i–V* curve supplies a value for the ohmic resistance of the fuel cell, the so-called area specific resistance (ASR). It accounts for the fact that fuel cell resistance scales with area, thus allowing different size fuel cells to be compared.

4. Results and discussion

4.1. Graphite rods

The graphite rods operated very well in the DCFC. The method in which they were manufactured allowed for reliable experiments to be conducted. Because of their stability, it was possible to run multiple types of experiments, changing the process variables without the rod degrading. The graphite rods left the electrolyte fairly clean after finishing an experiment, which showed that not much particulate carbon was dissolving into the electrolyte. Any carbon that was missing from the surface of the rod was, therefore, reacting with the hydroxide to form electrical power.

The maximum open-circuit voltage (OCV) from a graphite rod was 0.788 V. This value for the graphite rods was not as high as obtained from the coal-derived rods, as previously noted in literature. However, a higher current density is obtained from the graphite rods due to the increased current drawn which in turn, raises the maximum power density. A summary of the runs involving graphite fuel rods is given below in Table 2.

An example of results from one of the graphite runs is shown below in Fig. 5. This run was conducted at an operating temperature of 600 °C and an air flow rate of 0.50 SLPM. It is interesting to note that all of the graphite runs have the same shape for their

Table 2
Summary of results for runs using graphite fuel rods

Run	Open-circuit voltage (V)	Maximum current density (mA cm^{-2})	Maximum power density (W cm^{-2})	Area specific resistance (Ω cm^2)	Active surface area (cm^2)
1	0.751	230	0.066	2.91	50.5
2	0.767	207	0.068	2.75	49.5
3	0.779	175	0.065	2.74	50.5
4	0.788	105	0.048	2.50	54.5
5	0.757	133	0.057	2.00	51.9
6	0.760	170	0.073	1.60	51.9
7	0.773	183	0.062	2.60	51.9
8	0.735	185	0.048	3.00	51.9
9	0.770	197	0.084	1.60	51.9
10	0.729	214	0.062	2.20	51.9
17	0.705	107	0.041	2.20	41.3

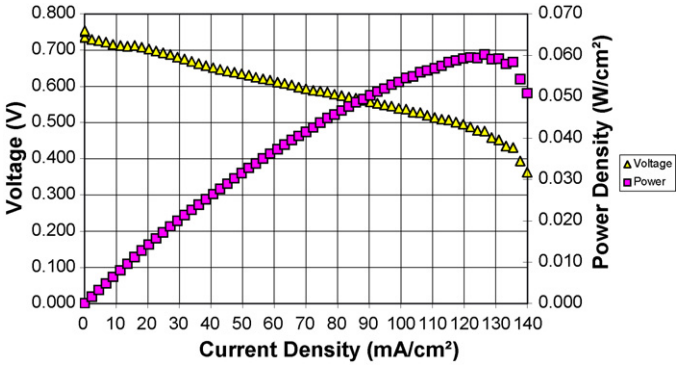

Fig. 5. Example of cell voltage and power density vs. current density for a graphite experiment subject to the operating conditions of Run #2. Air flow rate = 0.50 SLPM and $T = 600\,^{\circ}$C.

i–V curve. The curves all drop quickly near zero current due to the activation resistance. They continue to decrease in a linear fashion due to the ohmic resistance of the cell. Finally, the voltage decreases sharply at high currents due to the concentration or transport limitation being reached [11]. The fuel cell power density increases with increasing current density, reaches a maximum, and then falls at still higher current densities.

The graphite rods were very consistent during the many runs in which they were used. The data are reproducible when the same experimental conditions are used. As shown in Table 2, the range in OCV was less than ± 0.05 V. The reason for the slight differences between experiments is most likely due to resistances within the cell itself. Ohmic resistance (ASR) can occur from the electrode materials, mechanical connections within the cell apparatus, and even within the electrolyte itself. However, between each run the cell was dismantled and thoroughly cleaned prior to testing another fuel rod. Fresh electrolyte was used for every run.

4.2. Coal-derived rods

The results from the coal-derived carbon rods are shown in Table 3. As can be seen, the coal-derived rods produced a higher open-circuit voltage as compared to the graphite rods. This is because the molecular alignment in the coal-derived rods is not as organized as the graphite rods and the carbon is more accessible for reaction. Therefore, there are more active reaction sites on the coal-derived rods and hence these rods show a higher electrochemical activity. However, these rods did not produce a very large current density due to their high area specific resistance, as shown in Table 3.

Unlike the graphite rods, the coal-derived rods did not give stable and consistent operation. The rods seemed to physically degrade (broke, dissolved, etc.) in the cell. The degradation was traced to the selective and preferential attack of the binder carbon which holds the rod together. This is because the coke from the coal tar binder is more reactive than the coke in the rod. For example, the rod in Run #13 broke off at the electrolyte surface during the run. Moreover, after an experiment had been run, the electrolyte was seen to be quite black, indicating dispersed carbon in the electrolyte. There also seemed to be a carbon buildup around the surface of the molten electrolyte clinging to the surface of the cell body. This buildup also occurred at the point on the rod that was at the top surface of the electrolyte.

Table 3
Summary of results for runs using coal-derived fuel rods

Run #	Open cell voltage (V)	Maximum current density (mA cm^{-2})	Maximum power density (W cm^{-2})	Area specific resistance (Ω cm^2)	Active surface area (cm^2)
11	0.963	53	0.033	4.30	60.6
12	0.981	48	0.032	4.20	43.7
13	Rod broke off at electrolyte surface				
14	0.963	31	0.020	8.10	71.7
15	Rod did not survive experiment preparation				
16	1.044	35	0.024	7.55	66.5
18	0.972	38	0.026	4.20	65.2

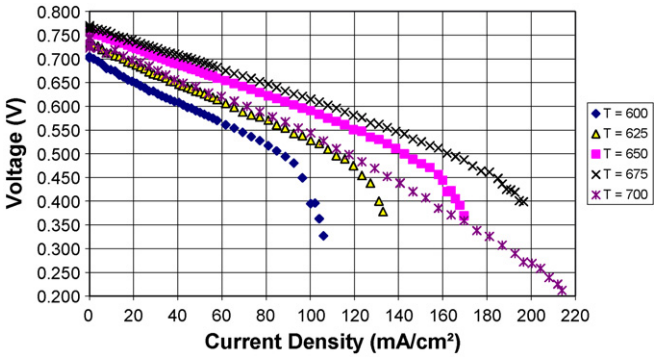

Fig. 6. Effect of temperature on cell voltage as a function of current density. Data taken from Runs #4, #5, #6, #8, and #10, at a flow rate of 0.5 SLPM while using a graphite rod.

Surprisingly, the well-fabricated GrafTech, Inc. baked rod (Run #18) did not show better results than the baked rods produced at WVU. This indicates that it was not the manufacturing method that caused the rods to show a lower performance, but the preferential attack of the coal tar binder pitch which was observed for both sets of baked rods.

The total current and power that was drawn with the coal-derived rods were much lower than that seen for the graphite rods. This is due in part to the higher ASR for the coal-derived rods which dissipates power due to ohmic heating.

4.3. Effect of temperature

During the tests with the graphite rods, the cell temperature was varied stepwise from 600 to 700 °C and the *i–V* scans were made. The results indicate that the increase in temperature clearly causes an increase in performance in the cell, as shown in Fig. 6 for the *i–V* scans. However, there is a maximum temperature at which the thermal effect ceases to increase performance. According to the data, it appears that the reaction is optimized at around 675 °C. Data at 700 °C show that the cell voltage is less, even though more current is drawn than at the lower temperatures.

The same can be seen for the power output in this case, as illustrated in Fig. 7. The maximum power is obtained at 675 °C after a trend of increasing performance. The power output at 700 °C is lower, and therefore, it appears that the optimum temperature for power output is also around 675 °C, even though more current is drawn at 700 °C.

Although the theoretical values of E° obtained for different temperatures in the Nernst Equation are similar, the values for E_{cell} obtained experimentally clearly show a strong temperature effect [12]. From, Eq. (5), it appears that the influence of temperature is dependant on the natural log of the ratio of the partial pressures of CO_2 and O_2. Assuming a well-mixed environment, a negative ratio of the concentration implies the partial pressure of CO_2 in the inlet gas is small compared to O_2. When this occurs, the cell voltage will increase with temperature, which is seen in the data from 600 to 675 °C. At the higher temperature, there may be more CO_2 produced in the cell, which would cause the voltage output to decrease at even higher temperatures, due to the ratio being positive.

$$E_{cell} = E^\circ - \frac{RT}{NF} \ln \frac{[CO_2]}{[O_2]} \quad (5)$$

It should be noted that this equation holds for C reacting with gaseous O_2 to make gaseous CO_2, a situation that is not present in these experiments. However, this equation is frequently cited in literature and may be relevant when using the concentrations of O_2 and CO_2 in the electrolyte [2].

4.4. Effect of air flow rate

The effect of the air flow rate into the cell influences the performance of the cell as shown below in Figs. 8–10. There is a clear peak at 0.50 SLPM where the maximum performance is obtained at 675 °C, as shown in Figs. 8 and 9, while the optimum performance at 600 °C appears to be at higher air flow rates, as shown in Fig. 10.

At a flow rate below the optimum air flow value (e.g., 0.25 SLPM), the optimum amount of air is not being supplied for the reaction. Referring to Eq. (5), supplying more oxygen into the system should cause the natural log of the ratio to be more negative, causing the cell voltage to increase.

At a flow rate above the optimum air flow value (e.g., 0.75 SLPM), the air is either flowing too quickly for the reaction to occur optimally, or it may be that the bubbles emanating from

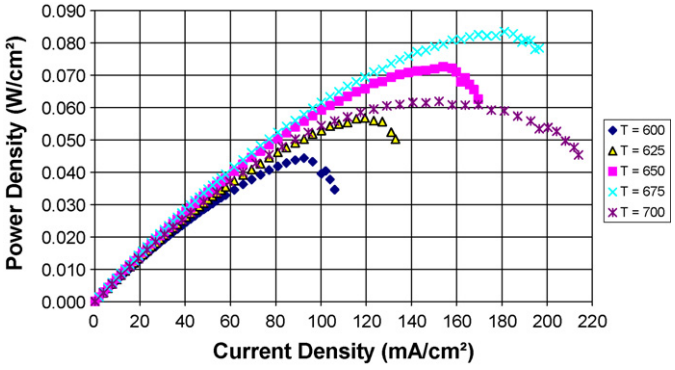

Fig. 7. Effect of temperature on power density as a function of current density. Data taken from Runs #4, #5, #6, #8, and #10, at a flow rate of 0.5 SLPM while using a graphite rod.

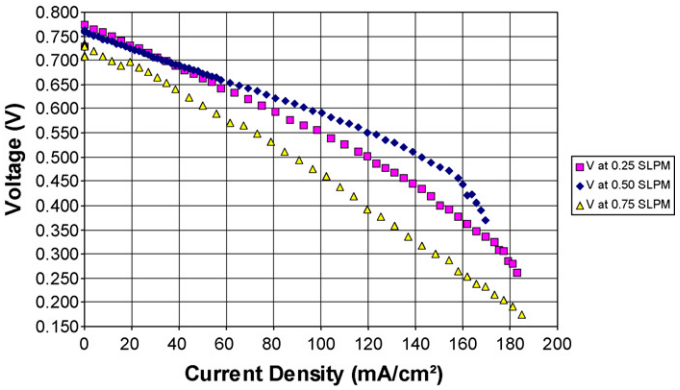

Fig. 8. Effect of air flow rate on cell voltage using a graphite rod at 675 °C.

Table 4
Summary of results by carbon fuel rod

Rod (Run #)	Maximum open-circuit voltage (V)	Maximum current density (mA cm^{-2})	Maximum power density (W cm^{-2})	Area specific resistance (Ω cm^2)
Graphite (1, 4, 9)	0.788 (4)	230 (1)	0.084 (9)	2.59
WVU baked (11, 16)	1.044 (16)	53 (11)	0.033 (11)	5.90
GrafTech baked (18)	0.972	38	0.026	4.20

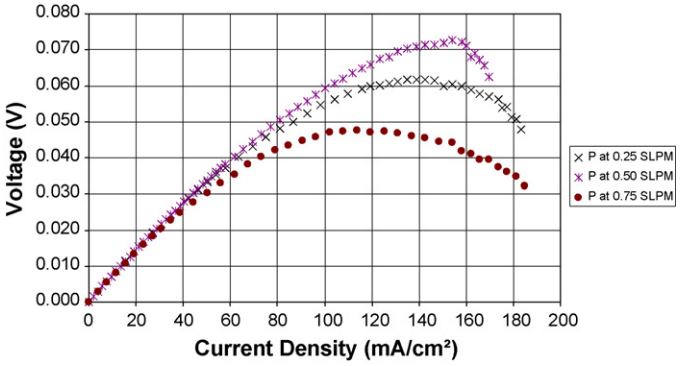

Fig. 9. Effect of air flow rate on power density using a graphite rod at 675 °C.

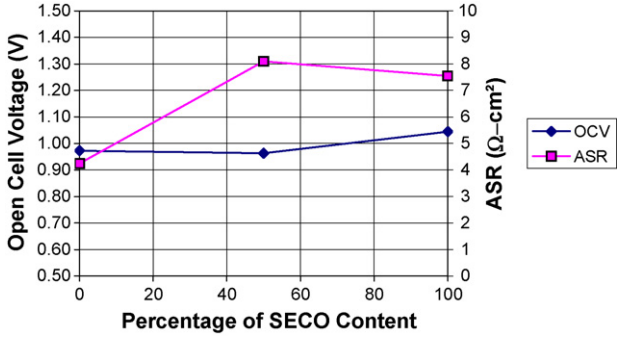

Fig. 11. Trends of open cell voltage and area specific resistance vs. percentage of SECO content.

the spider are too large. This causes poorer gas–solid contact at the cathode surface and hence inhibits the cathode reaction. It should be noted that the spider/cell design used here was not optimized with respect to gas–solid interaction. Thus, it seems for these runs with this cell design, the optimum air flow was found to be above 0.50 SLPM (Fig. 10).

4.5. Summary of effect of fuel rod composition

Table 4 is a summary of the main results obtained from the different fuels. The ASR is calculated as average values. The best voltage output was obtained using the WVU coal-derived rods, as was expected. The GrafTech baked rod also reached nearly 1.0 V. Recall that the standard potential for the oxidation of carbon is 1.01 V. The SECO rod recorded a voltage slightly over the standard potential, probably due to reactions of some impurities or the binder pitch used in the rod.

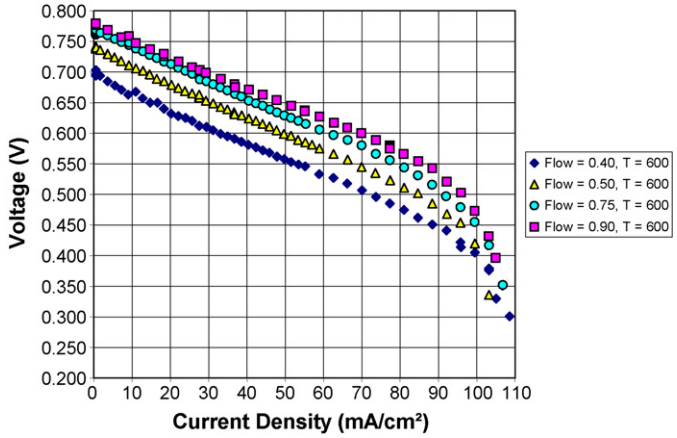

Fig. 10. Effect of air flow rate on cell voltage using a graphite rod at 600 °C.

The trends in the OCV and ASR versus SECO content for the SECO/PetCoke rods are shown below in Fig. 11. The OCV does not change appreciably overall, but it can be seen that the OCV is the highest at 100% SECO content. The OCV is the lowest where the ASR is at its maximum, as expected. There must, however, be other factors which account for the low OCV observed at 0% SECO content. Once again, the ohmic resistance hinders ionic and electronic conduction in the electrolyte and electrodes, and therefore, lowers cell voltage. Moreover, mechanical variation in the connections for the cell add other "non-chemical" resistances as pointed out above in Section 4.1.

5. Conclusions

Using carbon rods as a fuel source, the direct carbon fuel cell produced electricity as predicted. The following conclusions can be drawn from the work:

- Graphite rods were used to establish baseline performance of the DCFC. They provided reliable and reproducible data and ensured proper operation of the system.
- Coal-derived rods from blends of SECO and PetCoke were successfully tested in the system.
- The effects of temperature and air flow were investigated for graphite rods and showed that cell performance peaks at about 675 °C and 0.50 SLPM with NaOH as the electrolyte. Graphite rods had better long-term stability.
- The fuel cell performance was evaluated via *i–V* curves, which can be used to investigate different types of cell resistances. Graphite rods produced open-circuit voltages of up to 0.788 V and current densities up to 230 mA cm^{-2} while coal-derived

rods produced open-circuit voltages of up to 1.044 V and only 35 mA cm^{-2} in current density. The ASR for the graphite rods was found to be around 2 Ω cm^2 while that for the baked coal-derived rods was around 6 Ω cm^2.

- The fuel cell performance was evaluated by comparing plots of power densities versus the current density and noting the peak power output. Graphite rods produced peak power of about 0.084 W cm^{-2} while coal-derived rods were only able to produce 0.033 W cm^{-2} because of their higher ASR.
- Binder pitch is attacked preferentially in the reaction. Therefore, the baked coal-derived rods disintegrated over time in the electrolyte.
- GrafTech baked rods were tested to investigate whether the method of manufacture influenced the behavior of the coal-derived rods. As in the coal-derived rods, these baked rods did not show long-term stability due to the preferential reactivity of the binder pitch. Thus, the method of manufacture is not the main cause of the mechanical failure of the baked rods.

Acknowledgements

Ned Patton and Kevin Walter of SARA, Inc. are acknowledged for their assistance and guidance during this research.

References

[1] West Virginia Department of Commerce, Office of Miners' Health Safety and Training, http://www.wvminesafety.org/.
[2] N.J. Cherepy, R. Krueger, K.J. Fiet, A.F. Jankowski, J.F. Cooper, J. Electrochem. Soc. 152 (1) (2005) A80–A87.
[3] Jacques, William W., Method of converting the potential energy of carbon into electricity, Patent Number 555,511 Newton, MA (March 3, 1896).
[4] Blomen, J.M.J. Leo, Mugerwa, N. Michael, Fuel Cell Systems, Plenum Press, New York, 1993, pp. 22–23.
[5] R.D. Weaver, S.C. Leach, A.E. Bayce, L. Nanis, Direct Electrochemical Generation of Electricity from Coal, February 15, SRI, Menlo Park, CA, 1979.
[6] R.D. Weaver, L. Nanis, in: Proceedings third International Symposium on Molten Salts, Electrochem. Soc. 81–9 (1981) 316.
[7] NDT, Resource Center, http://www.ndt-ed.org/.
[8] K. Renganathan, J.W. Zondlo, E.A. Mintz, P. Kneisl, A.H. Stiller, Fuel Process. Technol. 18 (1988) 273–278.
[9] Saddawi, Abha, carbon fuels for the direct carbon fuel cell, Master's Thesis, Department of Chemical Engineering, West Virginia University, 2005.
[10] Hackett, Gregory, Evaluation of carbon materials for use in a direct carbon fuel cell, Master's Thesis, Department of Chemical Engineering, West Virginia University, 2006.
[11] A. Dicks, J. Larminie, Fuel Cell Systems Explained, second ed., John Wiley and Sons, New York, 2003 (Chapter 3).
[12] H.H. Lowry, Chemistry of Coal Utilization, vol. II, John Wiley and Sons, New York, 1945, pp. 1568–1573.